Journal of Hydroscience and Hydraulic Engineering
Vol. 13, No. 1, May, 1995, 47-61

EROSION AND TRANSPORT PROCESSES OF COHESIVE SEDIMENT IN DAM RESERVOIRS

By

Yuichi KITAMURA

Deputy Manager, Environmental Planning Division, Electric Power Development Co.,Ltd. (EPDC)
15-1,Ginza 6-chome,Chuo-ku, TOKYO 104, JAPAN

SYNOPSIS

This report describes an effective method for evaluating the erosion and transport processes of cohesive sediment in a dam reservoir and the outflow of turbid material when the water level of a reservoir falls down. Discussions are made on these phenomena by referring to actual observations in order to specify parameters that govern the erosion characteristics of cohesive sediment. A formula about erosion velocity of cohesive sediment is developed in terms of field experiments as well as of laboratory tests. The formula is applied to one-dimensional governing equations to predict the reservoir bed changes and turbidities of outflow water. The calculated results are compared with observed data.

INTRODUCTION

In recent years water quality of reservoirs has become important problems in the environmental management of reservoirs. It is put importance to the proper control of sediment and turbidity. Among various turbidity problems, the attention has been focused on the sediment suspension which arises during periods of excessively low water level, which happens in the period of a sediment flushing, an unusual dry season, and an improvement of the dam facilities. When water level falls, the bottom of reservoir is exposed partly. In this occasion, the shear velocity increases, and sediment erosion takes place. This eventually leads to turbid water problems (1), (2).

Reservoir sediment in deep region generally contains a great deal of fine sediment of less than 100 microns in diameter. Clays among these turbidity-causing particles are known to be cohesive. In discussing the turbid water problem due to erosion of reservoir sediment during periods of excessively very low water level, it is therefore necessary to evaluate the erosion velocity of such cohesive (fine) sediment.

CHARACTERISTICS OF DEPOSITED SEDIMENT, BED PROFILE AND TURBIDITY

Bed Profile and Characteristics of Sediment Observed in Ikehara Reservoir

In sedimentation process in a reservoir, sediment particles are accumulated according to a kind of sieving effect. The geometric characteristics of bed profile is produced, depending on particle size distribution of the inflow sediment, the amount of inflow, the water level, the reservoir shape, etc.

The longitudinal bed profiles of the Ikehara reservoir, which are original and measured in 1986, are respectively shown in Fig.1. The ratio of the sediment volume to the maximum storage capacity

of reservoir is only 1.1%, but a representative profile like a fore-set bed is formed around the minimum operating water level. The sediment sampling points along the main reach and tributaries in back water region are indicated in Fig.2, and the sediment particle size distribution curve of each sampling point is shown in Fig.3. It is found that the particle size of deposited sediment is affected very much by water depth. In the upstream region of reservoir, as shown in Fig.3, coarse sediment dominates in the sections No.49, 93 and 131, and fine sediment less than 100 microns in diameter prevail in the downstream of section No.35. These curves clearly show that the particle size of sediment is distinguished; relatively large particles, such as bed load deposited in the upstream of the fore-set bed and fine sediment, less than 100 microns in diameter, deposited in the downstream of it.

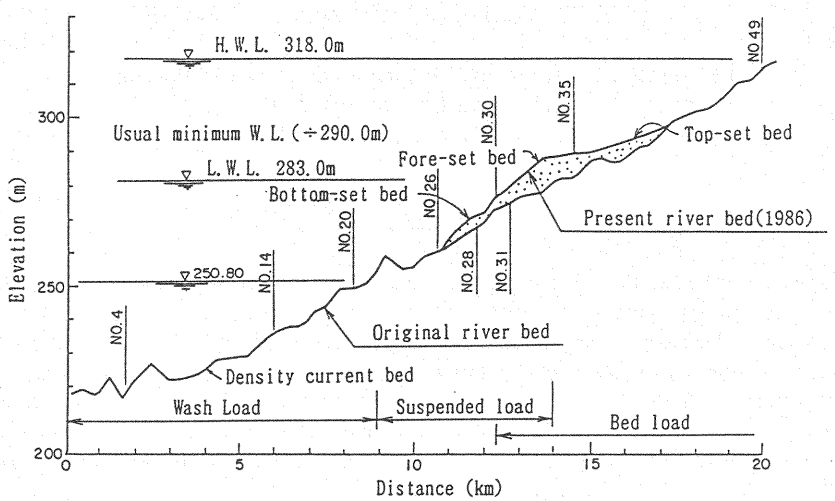

Fig.1 Longitudinal bed profile of Ikehara reservoir

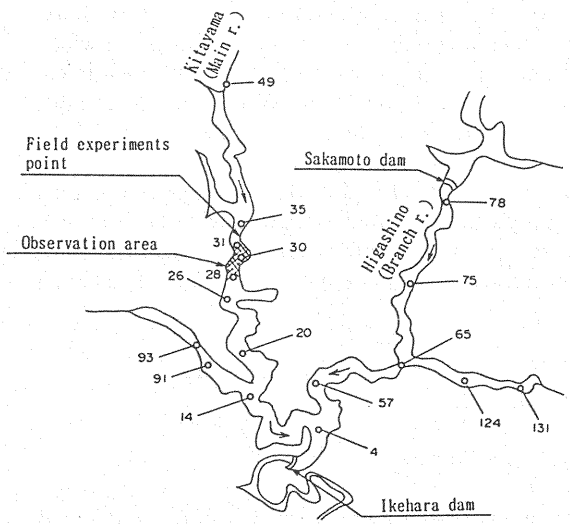

Fig.2 Sediment sampling points, and field experiments and observation area at Ikehara reservoir

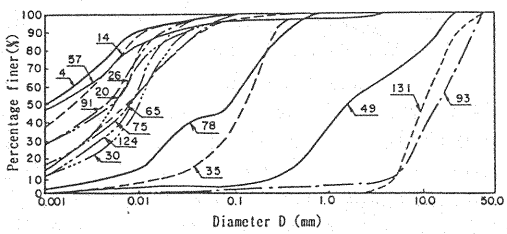

Fig.3 Sediment particle size distribution curves at Ikehara reservoir bed

Fine sediment can be divided into suspended load and wash load by areas; suspended load is mostly deposited in just downstream of the fore-set bed and wash load mainly in the further downstream until the dam site. Even in the upstream area, very fine sediment deposits into bed with coarse sediment (3). The source of the turbid material, therefore, exists in extended areas where the bed load and suspended load locally dominate.

In general, flow velocity or shear velocity is not large enough for re-erosion of deposited sediment. Thus, no turbid material run off under ordinary circumstances. However, when the water level falls down, the water flow becomes like that in a river. Thus the shear velocity increases, and sediment erosion may occur. In particular, exposure of the sediment downstream of the fore-set bed enhances erosion and transport of sediment. In such a manner, turbid material could be produced.

Turbidity Due to Erosion of Deposited Sediment at Funagira Reservoir

The Funagira power plant turbines were overhauled between January 10 and March 27, 1986. At the same time maintenance works of the flood discharge control gates were carried out by reducing the water level to about 15 m below an ordinary operating water level. It was the good opportunity for understanding sediment erosion of reservoir bed. Turbidity of flow water, discharge and changes of the reservoir bed elevation were measured and sediment materials were collected during the works (4).

The temporal variations of turbidities, discharges and water level are shown in Fig.4. The turbidity of outflow water increased remarkably as the water level decreased toward the lowest water level, reaching the maximum of 350 ppm just before the minimum water level was achieved. At that time the turbidity of inflow water was about 60 ppm. The turbidity of outflow water decreases to about 50 ppm on the following day and to about 20 ppm on the second day. Four to five days after the peak of turbidity of outflow, it became as same as that of inflow water.

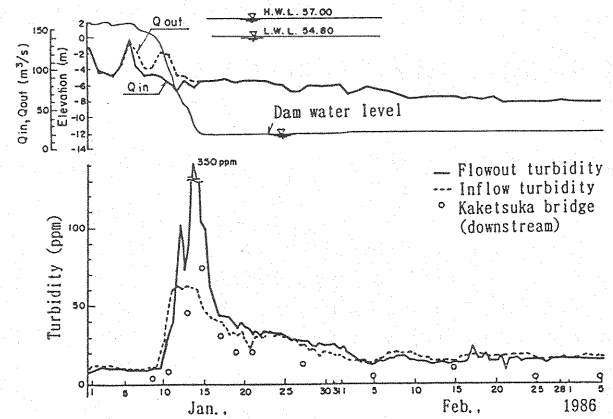

Fig.4 Temporal changes of turbidity discharge andwater level at Funagira reservoir

The changes of turbidity distribution in reservoir while the water level is reducing are shown in Fig.5. Particle size distribution curves of bed sediment collected before and after the fallen water level are shown in Fig.6. According to the results shown in these figures, the turbidity was higher around the upstream end of back water region at each stage and it became much higher as the water level decreased. Turbidity gradually decreases to the downstream, while it is almost uniform over depth. With attention focused on the changes of fine material constitution in bed sediment, almost all the fine sediment less than 100 microns in diameter were lost after the recession of water level as shown in Fig.6.

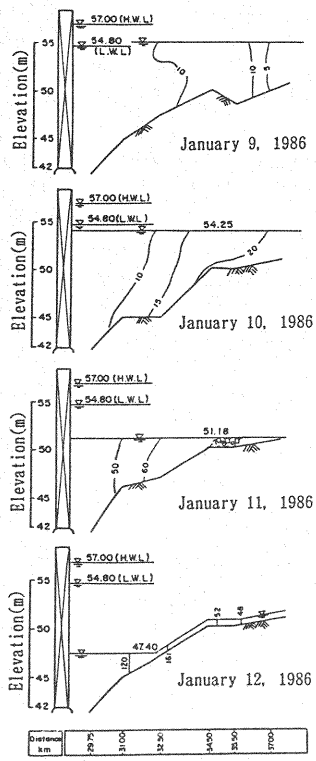

Fig.5 Turbidity distribution in Funagira reservoir

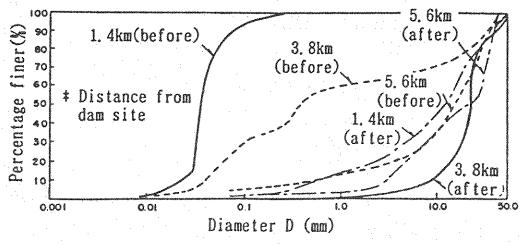

Fig.6 Sediment particle size distribution in Funagira reservoir (Before and after controlling water level)

EXPERIMENTS ON SEDIMENT EROSION AND SPECIFICATION OF EROSION VELOCITY

Resistance to Erosion and Erosion Velocity

As it was discussed earlier, turbid material is consisted of very fine sediment of smaller than 100 microns in diameter, which are highly cohesive and colloidal. If the clay mineral constituents are similar everywhere in nature, erosion resistance of sediment can be specified in terms of the fine sediment constitution, particle size of fine sediment, and saturation index of void water. The saturation index of reservoir bed sediment must be almost 100%. Thus, it could be simply described with the fine sediment content and particle size of fine sediment. If the representative particle size of fine sediment is larger, the amount of fine sediment tends to be less. The cohesion of sediment with larger particle size decreases, while due to the gravity force increases.

It is considered that critical shear velocity of initiation of fine sediment erosion is expressed by particle size of fine sediment, specific gravity of particle in water, acceleration of gravity and void ratio. Dimensional analysis gives a functional relation:

$$U_{*c}^2 / sgd = F_c(e) \qquad (1)$$

where U_{*c}=critical shear velocity; d=representative particle size; s=specific gravity of soil particles in water ($s=\sigma-1$); g=acceleration of gravity; and e=void ratio.

Erosion velocity, which is defined as the erosion depth in unit time, may depend on the shear velocity acting on the bed surface and its critical one. Herein, the following relation is assumed.

$$\frac{E}{U_*} = F_E\left(\frac{U_*^2 - U_{*c}^2}{U_{*c}^2}\right) \qquad (2)$$

where E=erosion velocity of fine sediment; U.=shear velocity.

If the functional relation concerning F_C and F_E are defined unconditionally, the erosion velocities can be evaluated. However, there are many uncertainties, such as physical and chemical conditions of the fine sediment. At present, field test or flume test is one of useful methods to specify Eqs.(1) and (2).

Experiment on Erosion Velocity

As indicated in studies by Otsubo (5), (6), erosion phenomena of fine sediment can be described quantitatively if the problem is handled by experiments. Thus, experiments to evaluate erosion velocity were carried out both in the field and in the laboratory. Field experiments were conducted at a plateau of the Ikehara reservoir. This plateau is ordinarily submerged, but is exposed during an usual dry season. A very flat area was chosen as the experimental site, and two waterways, 10 m long, were excavated there. The one had a trapezoidal cross section (1:1 gradient) and the other had a rectangular cross section 30 cm wide and 10 to 20 cm deep. Three kinds of constant flow discharge were employed for each water way. Clear water was supplied at the upstream end of the waterway by using a pump. Various measurements, such as flow velocity, cross-sectional shape, waterway gradient, and waterway width were made, and sediment concentration was measured at three cross sections.

In the laboratory experiments the sediment taken out at the plateau and a coarser sediment taken out at further upstream (see Fig.2) were employed. The experimental channel shown in Fig.7 was used. It is 30 cm wide, 30 cm deep, and 9.5 m long with a rectangular-section. The side wall of its middle reach, 5.8 m long, was made of transparent acrylic panel for observations. The bed slope was adjustable by use of jacks. Part of the upstream reach was made deeper to stabilize a flow.

To begin with the experiment, sediment material was mixed with water and then silted in still water. The porosity of the sediment was adjusted by changing the leaving time or removing the supernatant water and drying in the air. Thus, initial bed conditions were made. The particle size distribution curves of the materials used for these experiments are shown in Fig.8. As shown in

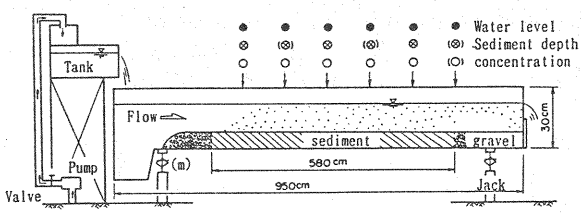

Fig.7 Laboratory experiment set-up

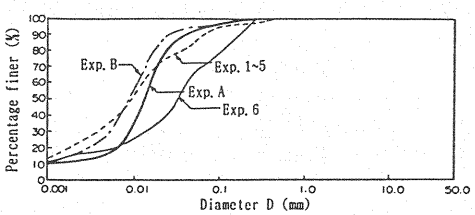

Fig.8 Sediment particle size distribution curves of sediment employed in flume tests

Fig.8, each material contains a large amount of fine sediment less than 100 microns in diameter. In each test, water was supplied at constant rate, and measurements were performed for velocity profiles, water depth, depth of bed material, sediment concentration of flow water. In addition the vertical

profiles of sediment concentration were measured at five cross sections. The experimental conditions are shown in Table 1, where γ=porosity; T=water temperature; Q=flow discharge; q=unit flow discharge; i=bed slope and i_e=energy gradient.

Table 1 Experiment conditions

Exp No	d_{60}(mm)	λ	T(℃)	Q(l/s)	q(cm²/s)	i	i_e
*A- 1- 3	0.015	0.62	10.0	2.0- 8.0	121- 329	1/25.5	———
B- 1- 3	0.010	0.66	10.0	2.0- 6.0	57- 207	1/63-1/44	———
*1- 1- 5	0.013	0.84-0.87	14.0-20.5	9.0-12.0	300- 400	———	0.0002-0.0007
2- 1-11	0.013	0.77-0.78	6.5-20.0	13.0-34.5	433-1150	1/420	0.0008-0.0064
3- 1- 5	0.013	0.76-0.79	15.5-18.0	15.0-23.0	500- 767	———	0.0021-0.0036
*4- 1- 5	0.013	0.74	13.2	16.0-24.0	533- 800	———	0.0017-0.0036
5- 1- 5	0.013	0.73	11.0-11.2	18.0-33.0	600-1100	———	0.0008-0.0025
6- 1- 7	0.040*	0.77	9.5	20.0-32.0	667-1093	1/390.1/180*	0.0004-0.0062

Note 1 : Experiments A and B are field tests and Experiments 1 to 6 are laboratory tests.
Note 2 : Sediment was left in the water in the experimnets 1 to 3 and was dried in the air without supernatant in the experiments 4 to 6.
Note 3 : The upstream sediment was only used in the experiment 6.

Experimental Results and Discussion

The erosion velocity E was determined from the following equation:

$$E = \frac{1}{\sigma} \frac{C(x+\Delta x) - C(x)}{\Delta x} \frac{Q}{B} \tag{3}$$

where σ=specific gravity of soil particle; C=fine sediment concentration inflowing water (by weight); Q=flow discharge; B=flow width; x=coordinate system along flow direction.

The relation between square of shear velocity and erosion velocity is shown in Fig.9. Herein, U_* is the shear velocity. The data, which is obtained from field and laboratory experiments, is classified into several groups according to the difference of void ratio. In addition the field data, which is recently obtained from observing actual reservoir bed erosions and discussed later, is also plotted. As these data indicate, the erosion rate increases sharply with the increase of U_*^2. It is expected that sediment concentration of flowing water becomes negligibly small as the erosion velocity reduces to the order of magnitude 10^{-6} cm/s. From a practical view point, therefore, shear velocity giving the erosion velocity of about 10^{-6} cm/s, which is the turbidity meter detection limit, is employed as the critical shear velocity for erosion. In Fig.10, data of the critical shear velocity are shown in order to test a functional form of Eq.(1). According to the results, the nondimensional critical shear velocity for erosion could be described in terms of void ratio as follows;

$$U_{*c}^2 / sgd = a e^{-b} \qquad (a=20-40,\ b=2) \tag{4}$$

can be expected.
where a=empirical constant; and b=empirical constant.

In Fig.11, a nondimensional expression of erosion velocity is shown in a form of Eq.(2), in which data are the same as those in Fig.9. The results obtained from field and laboratory experiments fall almost on the same lines, although the laboratory data indicate a slightly greater value of n than the others. The equation is lead by Fig.11:

$$\frac{E}{U_*} = N\left(\frac{U_*^2 - U_{*c}^2}{U_{*c}^2}\right)^n \qquad \begin{pmatrix} N=4*10^{-5},\ n=1.5 & \textit{for maximum} \\ N=1*10^{-1},\ n=1.0 & \textit{for minimum} \end{pmatrix} \qquad (5)$$

where N=empirical constant; and n=empirical constant.

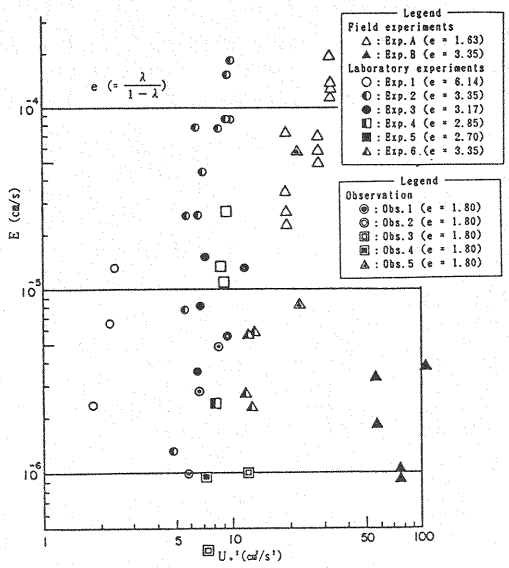

Fig.9 Relation between shear velocity and erosion velocity

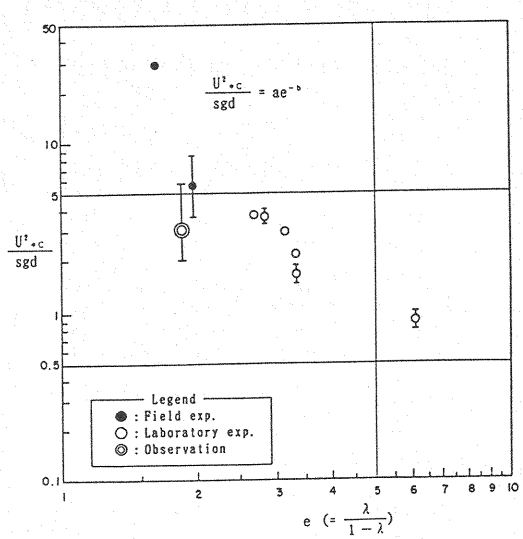

Fig.10 Relation between void ratio and dimensionless critical shear stress

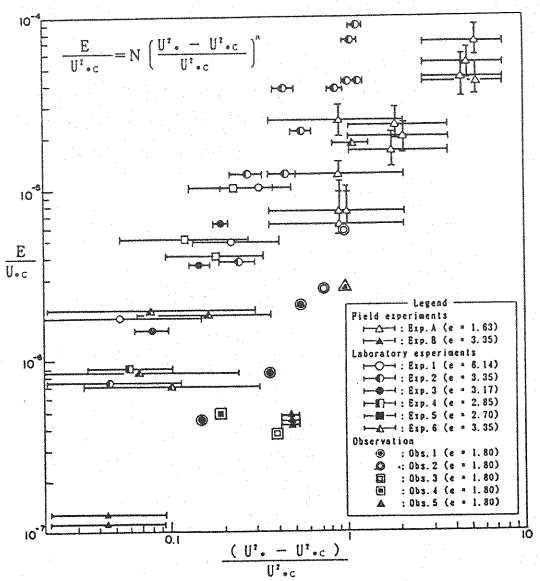

Fig.11 Relation between effective shear velocity and nondimensional erosion velocity

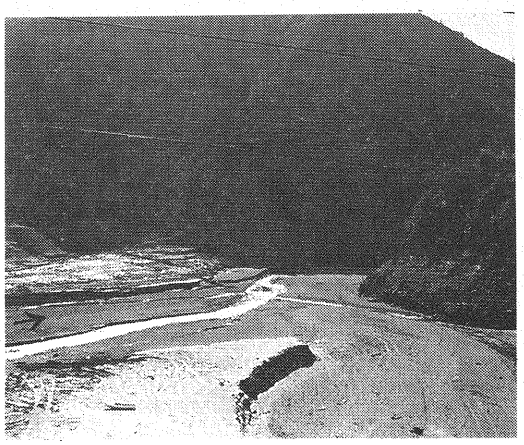

Photo 1 Erosion of sediment (Ikehara reservoir)

From September 1990 to June 1991, the existing intake facility was changed into a surface withdrawal intake at Ikehara reservoir for reducing turbidity problem. The water level of the reservoir was fallen down about 30 m than normal L.W.L. (E.L.283 m) during the reconstruction. At that time, the lowest water level was E.L.250.8 m. Using this opportunity (Photo 1), the observation was done for measuring width of current, cross-section, bottom level changing, velocity, turbidity, conductivity, water temperature.

Table 2 shows erosion velocity which was determined from the observation. The obtained critical shear stress and erosion velocity from the field observation are added to Figs.9, 10 and 11. They are fitting well with the field and laboratory experiments data and can be predicted by Eqs.(4) and (5).

Table 2 Erosion velocity specified by observed data

date	Section No.	ρ/ρ_s	λ	e	q (m^2/s)	dC/dX	E (cm/s)	U_*^2 (cm^2/s^2)
Dec. 27, '90	28-29	0.37	0.64	1.8	0.326	0.380	4.56×10^{-6}	7.84
	29-30	0.37	0.64	1.8	0.235	0.205	1.78×10^{-6}	6.82
	30-31	0.37	0.64	1.8	0.186	0.146	1.01×10^{-6}	5.81
Jan. 22, '91	28-29	0.37	0.64	1.8	0.360	1.019	13.57×10^{-6}	10.81
	30-31	0.37	0.64	1.8	0.276	0.564	5.76×10^{-6}	9.34
Feb. 26, '91	28-29	0.37	0.64	1.8	0.488	0.056	1.01×10^{-6}	11.22
	29-30	0.37	0.64	1.8	0.400	0.021	0.31×10^{-6}	7.08
Mar. 20, '91	29-30	0.37	0.64	1.8	0.369	0.068	0.93×10^{-6}	7.12
Mar. 26, '91	30-31	0.37	0.64	1.8	0.366	0.645	8.73×10^{-6}	23.52

MATHEMATICAL MODEL FOR RESERVOIR BED CHANGES AND SEDIMENT CONCENTRATION OF FLOW WATER

A schematic of sediment erosion, transport and deposition for the area, where bed load or wash load is the main constituent at certain points in time, is shown in Fig.12. In the area dominated by bed load, the outflow of turbid material mostly originates with beginning of bed load erosion, and almost no turbid material comes from the downstream area, where eroded bed load had accumulated on reservoir bed. While in the area dominated by wash load, turbid material can be produced due to bed erosion.

Equations Describing Reservoir Bed Changes

An one-dimensional mathematical model consists of five equations; mass and energy conservation, conservation of reservoir bed sediment, particle size specific conservation for sediment discharge rate, and sediment particle size distribution over reservoir bed (7). These are then solved for a particular set of boundary conditions. The equations are described appropriately as follows.

The mass conservation of flow water is as follows.

$$\frac{\partial A}{\partial t} + \frac{\partial Q}{\partial x} = 0 \qquad (6)$$

where A=cross-sectional area of current; and Q=flow discharge.

The conservation equation of mean flow energy is;

$$\frac{1}{g}\frac{\partial V}{\partial t}+\frac{1}{2g}\frac{\partial}{\partial x}V^2+\frac{\partial h}{\partial x}+\frac{\partial Z_b}{\partial x}=-i_e \tag{7}$$

where h=average depth; Z_b=reservoir bed level; and i_e=energy gradient.

The equation of conservation of reservoir bed sediment consisting of mixture of bed load and wash load, is adopted for calculation of reservoir bed change.

$$\frac{\partial Z_b}{\partial t}=-\frac{1}{(1-\lambda)B_b}\left[\sum_{i=1}^{J}\frac{\partial B_s q_{bi}}{\partial x}+\frac{\partial B_s q_w}{\partial x}\right] \tag{8}$$

where q_{bi}=bed load rate with d_i component of particle size; q_w=wash load rate; λ=porosity; B_b=reservoir bed width; B_s=effective reservoir bed width for sediment transport; and J=division number of bed load. The following conditions are adapted to Eq.(8) for the each area, where bed load or wash load is dominated over reservoir bed:

$$\begin{aligned} &U_* < U_{*ci} \ : \ \frac{\partial B_s q_w}{\partial x}=0 \qquad (\Sigma f_{bi} > f_w) \\ &U_* < U_{*cw} \ : \ \frac{\partial B_s q_{bi}}{\partial x}=0 \qquad (\Sigma f_{bi} < f_w) \end{aligned} \tag{9}$$

where U_{*ci}=critical shear velocity of particle size class, d_i; and U_{*cw}=critical shear velocity of wash load (fine sediment). Herein, U_{*cw} is calculated by Eq.(4).

To calculate bed load discharge rate q_{bi}, the formula presented by Ashida and Michiue (8), expressed by Eq.(10), is applied;

$$\frac{q_{bi}}{\sqrt{(\sigma-1)gd_i^3}}=17 f_{bi}\tau_{*ei}^{3/2}\left(1-\frac{\tau_{*ci}}{\tau_{*i}}\right)\left(1-\frac{U_{*ci}}{U_*}\right) \tag{10}$$

$$(\Sigma f_{bi}+f_w=1)$$

where f_{bi}=content rate of particle size class, d_i, in surface of reservoir bed layer; f_w = sediment content of wash load; τ_{*ei} = nondimensional effective shear stress on particle size class, d_i; τ_{*i}=nondimensional shear stress on particle size class, d_i; and τ_{*ci} = nondimensional critical shear stress on particle size class, d_i.

Here, U_{*ci} is given as follows according to the works of Egiazaroff (9) and Ashida and Michiue (8):

$$\begin{aligned} &\frac{U_{*ci}^2}{U_{*cm}^2}=0.85 , && \left(0.4 \geq \frac{d_i}{d_m}\right) \\ &\frac{U_{*ci}^2}{U_{*cm}^2}=\left(\frac{\log 19}{\log 19\, d_i/d_m}\right)^2\frac{d_i}{d_m} , && \left(0.4 < \frac{d_i}{d_m}\right) \end{aligned} \tag{11}$$

where U_{*cm}=critical shear velocity for a mean-sized particle calculated with Shields diagram.

To calculate wash load discharge rate q_w the following equation is used.

$$\frac{\partial B_s q_w}{\partial x} = B_s f_w E - B_b \alpha W_0 C \tag{12}$$

where w_0=falling velocity of wash load; and α=coefficient.

Temporal variation of particle size distribution over the reservoir bed in the case that bed load and wash load are relevant can be described by using Hirano's concept of a particle exchange layer (10). It is assumed that the top surface of the reservoir bed is an exchange layer, as shown in Fig.13, and that the representative particle size in this exchange layer is d (the representative particle size of the bed load multiplied by k). Denoting the ratios of bed load and wash load at the surface are f_{bi} and $f_w(\Sigma_i f_{bi} + f_w = 1)$, respectively, equations for f_{bi} and f_w can be written as follows.

$$\frac{\partial f_{bi}}{\partial t} = -\frac{1}{K_d B_b (1-\lambda)} \frac{\partial (B_s f_{bi} q_{bi})}{\partial x} - \frac{f_{bi*}}{K_d} \frac{\partial Z_b}{\partial t} \tag{13}$$

$$\frac{\partial f_w}{\partial t} = -\frac{1}{K_d (1-\lambda)} \left(f_w E - \alpha w_0 C \right) - \frac{f_{w*}}{K_d} \frac{\partial Z_b}{\partial t} \tag{14}$$

$$\partial Z_b/\partial t > 0 \qquad f_{bi*} = f_{bi}\ ,\ f_{w*} = f_w$$
$$\partial Z_b/\partial t < 0 \qquad f_{bi*} = f_{boi}\ ,\ f_{w*} = f_{w0}$$

where f_{b0i}, f_{w0}=content of bed load and wash load in the lower layer $(\sum_i f_{b0i} + f_{w0} = 1)$; and K_d=thickness of the exchange layer.

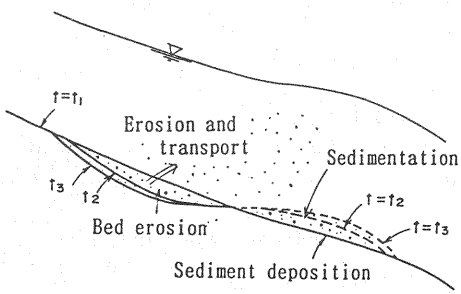

Fig.12 Sketch of bed erosion and sediment deposition

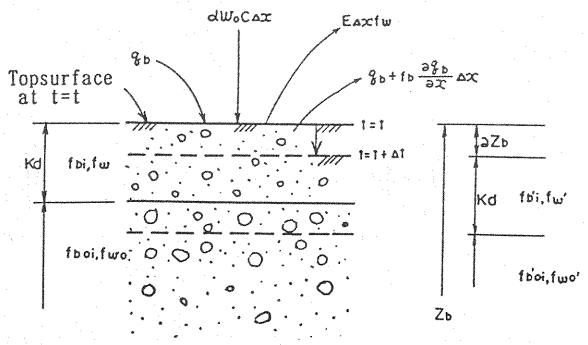

Fig.13 Definition sketch

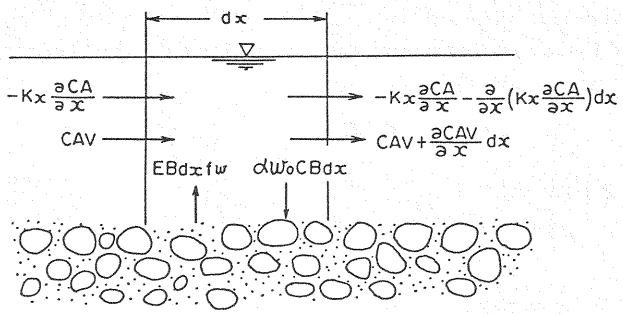

Fig.14 Schematics of mass conservation of fine sediment

Equation Describing Sediment Concentration in Flow Water

The budget of wash load in flow water with bed erosion and deposition is shown in Fig.14. Referring this figure, the conservation equation of wash load for the area where turbid material originates is described as follows.

$$\frac{\partial C}{\partial t}+V\frac{\partial C}{\partial x}=\frac{B_s E f_w}{A}-\frac{B_s \alpha w_0 C}{A}+\frac{\partial}{\partial x}\left(K_x\frac{\partial C}{\partial x}\right) \tag{15}$$

where K_x=dispersion coefficient.

APPLICATION OF MATHEMATICAL MODEL

The equations describing the reservoir bed change and the sediment concentration, were applied to the Ikehara reservoir. The numerical factors necessary for calculation are listed in Table 3. The dispersion coefficient is specified in terms of the equation: K_x = 500U.h (Iwasa, Aya, et al, (11)). The ratio of turbid material content refers to particle size of less than 100 microns in diameter. The water level of Ikehara reservoir was artificially fallen from E.L.283.0 m (L.W.L.) to E.L.240.0 m, which is shown in Fig.15. In the calculation, the daily average inflow discharges measured in 1974 was applied. The inflow and runoff discharge are shown in the same figure, too.

Table 3 Conditions of calculation

Item	Contents
Bed slope	Longitudinal bed shape in 1986 (See Fig.1)
Cross-sectional shape	Trapezoidal profile (1:3.6). River bed width (B_* = 60 m)
Specific gravity of soil	σ = 2.65
Porosity	λ = 0.65
Manning's resistance	n = 0.035 s/m$^{1/3}$
Sedimentation rate	W_0 = 0.7 m/day
Thickness of exchanging layer	K_d = 50 mm
Erosion velocity	a = 20 b = 2 in Eq.(4). N = 4×10^{-4} n = 1.5 in Eq.(5)
Particle size	d_m = 0.012 mm. d_{*1} = 1 mm. d_{*2} = 40 mm
Sediment content	f_m = 60%. f_{*1} = 35%. f_{*2} = 5%
Initial condition	t = 0 C = $C_0(x)$ = 0.0. H = H_{dam} (0) = 283 m
Boundary condition	x = 0 Q = $Q_{in}(t)$. C = $C_{in}(t)$. q_* (t) = 0.0
	x = L H = H_{dam} (t) dC/dt = 0. dq_*/dt = 0
Calculation period	Nov. 5, 1974 — Jan. 10, 1975

Note 1 : x = 0, L show upstream and downstream boundary.

The calculated results of turbidity at the inflowing section and outflowing water of the reservoir are shown in Fig.16. The result shows that during the period of decreasing water level, turbidity increases to a concentration of hundreds of ppm, even when the discharge is small. The calculated

results of relation between discharge and inflow turbidity is shown in Fig.17. The results are classified according to the period of falling water level, but from this figure the process of armoring is not clear.

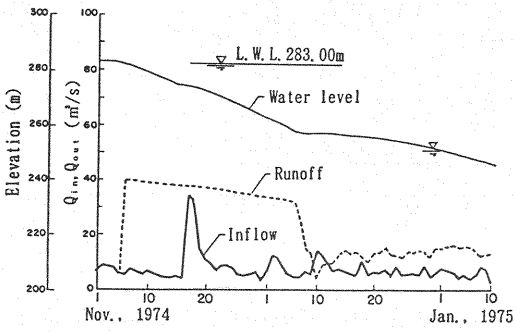

Fig.15 Calculated water level during the gate operation

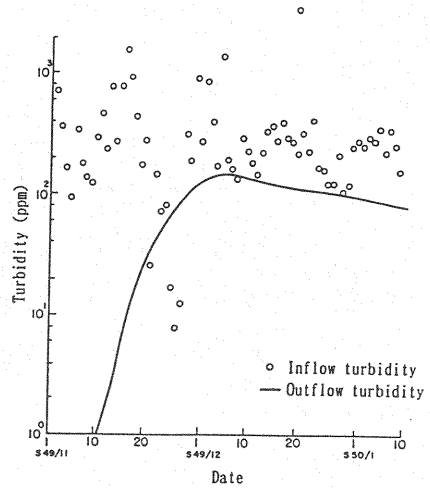

Fig.16 Calculated results of turbidity at the inflowig section and outflowing water of Ikehara reservoir

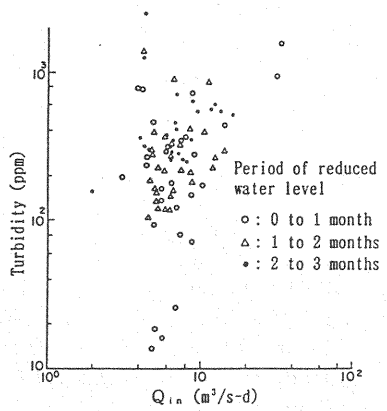

Fig.17 Relation between water discharge and turbidity at inflow point

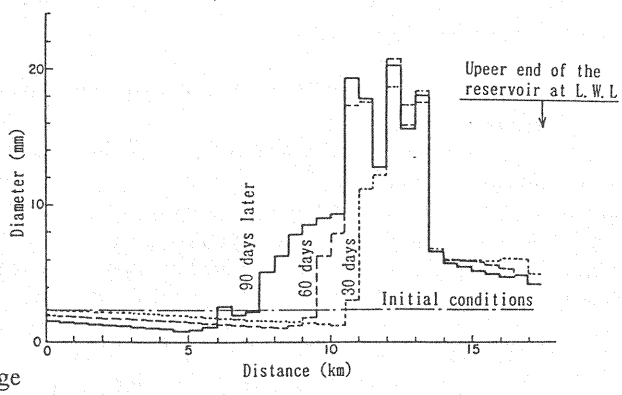

Fig.18 Average particle size of sediment at the surface layer of reservoir bed

The average particle size and turbid material content of sediment at the surface layer are shown in Figs.18 and 19. In Fig.18, the average particle size at the upstream the region of reservoir tends to be coarse as the water level falls and the armoring begins with the lapse of time. Such an armoring phenomena is representative at the downstream region of the fore-set bed. It is also shown in Fig.19 that the turbid material runs off from the upper region of the reservoir bed with the lapse of time.

The comparison between predicted and observed concentration of turbidity during lower water level are shown in Fig.20. The inflow concentration at the upper region of the reservoir became a few thousands ppm, and decreased after 4 months later. The observed outflow concentration is larger than predicted one, because there was a flood and the turbidity of reservoir became about 80 ppm just before falling water level. If it is taken into consideration of the initial turbidity as 80 ppm, the predicted concentration would agree well with observed one. The parameters employed in this calculation is listed in Tables 3 and 4.

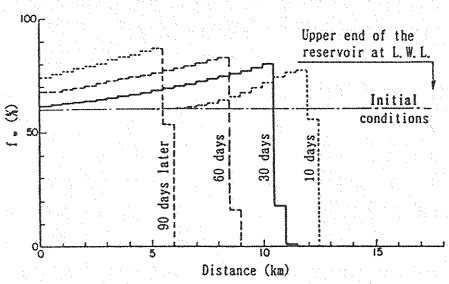

Fig.19 Turbid material content of sediment at the surface layer of reservoir bed

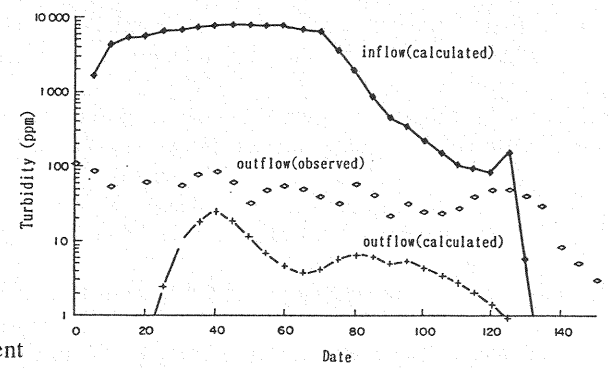

Fig.20 Comparison between calculated and observed fine sediment concentration during lower water level

Table 4 Parameters employed in the calculation

Item	Contents
Bed slope	i = 1/200
Cross-sectional shape	Trapezoidal profile (1:1.375). River bed width (B_s = 80 m)
Sedimentation rate	W_s = 0.4 m/day
Erosion velocity	a = 10 b = 2 in Eq.(4). $N = 0.3\times10^{-6}$ n = 1.0 in Eq.(5)
Particle size	d_* = 0.015 mm. d_{*1}-d_{*7} = 0.2. 0.4. 1. 2. 5. 10. 20 mm
Sediment content	f_* = 80%. f_{*1}-f_{*7} = 10. 5. 1. 1. 1. 1. 1 %
Calculation period	Nov. 11. 1990 — Apr. 10. 1991

CONCLUSION

The results obtained in this paper are summarized:

(1) From measurements at the Funagira reservoir, the erosion of deposited sediment certainly brings about a turbid water problem, though it may not last long. When a water level of a large reservoir is fallen, highly turbid water will be produced for an extended period.

(2) The functional relation, such as Eqs.(1) and (2), for the fine sediment erosion and specification of erosion velocity have been discussed. The empirical relation is proposed based on results in the field tests and the laboratory ones.

(3) The mathematical model, for the bed changes and the sediment concentration of flow water in a reservoir, where bed load and wash load dominate, are formulated.

(4) The mathematical model was applied to the case of falling water level in a reservoir. The calculated results described well the erosion and transport phenomena in a reservoir.

(5) The observation data about the actual bed erosion, which was conducted at the Ikehara reservoir during the reconstruction of intake gate, shows the good relation and fitting to the equations such as Eqs.(4) and (5). The comparison between calculated and observed data about turbidity of outflow water was made and those were founded to be fitting well.

Finally the author gratefully acknowledge the advice of Prof., Dr. Egashira, Ritumeikan University in preparing this paper.

REFERENCES

1. Electric Power Central Research Institute and Ministry of International Trade and Industry : Research on hydraulic power environmental security technology 1986, March 1987. (in Japanese)
2. Ashida K. and Egashira S. : Analysis on yield and transport mechanism of turbid materials in reservoir, a case study of Nagayasuguchi dam reservoir, Disaster Prevention Research Association, March 1982. (in Japanese)
3. Ashida K., Egashira S., Kanayashiki T., and Ogawa Y. : Yield processes of wash load in stream channels, Annuals, Disaster Prevention Research Institute (DPRI), Kyoto University, No.23 B-2, 1980. (in Japanese)
4. Electric Power Development Co.,Tenryu Power Plant : Report on water quality of Funagira dam during low water levels, May 1986. (in Japanese)
5. Otsubo K. and Muraoka K. : Study on the pick-up rate of cohesive bed material, Proc. 26th Jap. Con. on Hydraulics, 1982. (in Japanese)
6. Otsubo K. and Muraoka K. : Estimation of resuspension rate cohesive sediments by currents, Proceedings of JSCE No.375, 1986. (in Japanese)
7. Japan Society of Civil Engineers : Hydraulic formula handbook 1985 version, p.230. (in Japanese)
8. Ashida, K. and Michiue, M. : Study on Hydraulic resistance and bed-load transport rate in alluvial streams, Proc. JSCE, No.206, 1972. (in Japanese)
9. Egiazaroff, I. V. : Calculation of nonuniform sediment concentrations, Proc. ASCE, HY 4, 1965.
10. Ashida K. and Okabe T. : On the prediction model of reservoir sedimentation, Annuals, DPRI, Kyoto University, No.25 B-2, 1982. (in Japanese)
11. Iwasa, Y., Aya, S., Fujita, K. and Hoaoda, T. : Mass transfer processes in open-channel flows, Annuals, DPRI, Kyoto University, No.25 B-2, 1979. (in Japanese)

APPENDIX-NOTATION

a	= empirical constant;
A	= cross-sectional area of current;
B	= flow width;
b	= empirical constant;
B_b	= reservoir bed width;
B_s	= effective reservoir bed width for sediment transport;
C	= fine sediment concentration in flowing water (by weight);
d	= representative particle size;
e	= void ratio;
E	= erosion velocity of fine sediment;
f_{b0i}, f_{w0}	= content rate of bed load and wash load in the lower layer;
f_{bi}	= content rate of particle size class, d_i in surface of reservoir bed layer;
f_w	= sediment content of wash load;
g	= acceleration of gravity;
h	= average depth;
i_c	= energy gradient;
J	= division number of bed load;
K_d	= thickness of the exchange layer;
Kx	= dispersion coefficient;
N	= empirical constant;
n	= empirical constant;
Q	= discharge;

q_{bi} = bed load rate with d_i component of particle size;
q_w = wash load rate;
s = specific gravity of soil particles in water ($s=\sigma-1$);
U_* = shear velocity;
U_{*c} = critical shear velocity;
U_{*ci} = critical shear velocity of particle size class, d_i;
U_{*cw} = critical shear velocity of wash load (fine sediment);
U_{*cm} = critical shear velocity for a mean-sized particle;
w_0 = falling velocity of wash load;
x = coordinate system along flow direction;
Z_b = reservoir bed level;
α = coefficient;
λ = porosity;
σ = specific gravity of soil particle;
τ_{*ci} = nondimensional critical shear stress on particle size d_i;

(Received June 14, 1994; revised May 10, 1995)